Available online at http://scik.org
Commun. Math. Biol. Neurosci. 2026, 2026:15
https://doi.org/10.28919/cmbn/9720
ISSN: 2052-2541

MATHEMATICAL MODEL ANALYSIS OF STAGES OF CERVICAL CANCER WITH THE SIDE EFFECT HEMATOLOGICAL TOXICITY IN RADIO-CHEMOTHERAPY

DOUNIA KHALOUQI*, MARYEM EL KARCHANI, NADIA IDRISSI FATMI

LIPIM, ENSAK, Sultan Moulay Slimane University, Beni Mellal, Morocco

Abstract. Cervical cancer is the fourth most common cancer in women worldwide. Cancer treatments are often used to kill or remove tumors or metastases, reduce the risk of recurrence, and slow the development of tumors or metastases. They are also used to prevent and manage symptoms and complications caused by the disease and its treatments, ensuring the best possible quality of life. However, the effects of cancer treatments on patients are not always positive. The treatment of cervical cancer using a combination of radiotherapy and chemotherapy affects red and white blood cells as well as plasma. These side effects, known as hematological toxicity, led us to construct a mathematical model based on a population of hospitalized cervical cancer patients. This population is divided into five sub-populations classified according to disease stages, and the model is built using a system of differential equations. We analyzed the equilibrium points and performed stability analysis to study the population's dynamics over time. Finally, we conducted numerical simulations to verify the results of the analysis.

Keywords: cervical cancer; cancer stage; hematological toxicity; mathematical model; model analysis; numerical simulation.

2020 AMS Subject Classification: 91-10, 35A35, 34A30.

*Corresponding author

E-mail address: douniakhalouqi272@gmail.com

Received December 01, 2025

1. INTRODUCTION

Cervical cancer is characterized by abnormal, anarchic, and autonomous cell proliferation that destroys the cervix through local and distant invasion. According to the World Health Organization (WHO), cervical cancer is the fourth most common cancer in women worldwide, with approximately 660,000 new cases and 350,000 deaths linked to the disease in 2022 [23]. About 94% of these deaths occur in poor, low-, and middle-income countries. Cervical cancer mortality rates are particularly high in sub-Saharan Africa, Central America, and Southeast Asia [23]. In Morocco, cervical cancer is a public health issue with a high mortality rate. It is the second most common cancer affecting Moroccan women after breast cancer, with approximately 2,165 new cases and 1,199 deaths annually [1]. This situation reflects significant inequalities due to insufficient access to national services for human papillomavirus (HPV) vaccination, cervical cancer screening, and treatment, as well as the impact of social and economic determinants.

Cervical cancer is classified into two main types. The first type is squamous cell carcinoma, which accounts for almost 90% of cervical cancers. This type develops from the cells of the ectocervix. The second type is cervical adenocarcinoma, which originates in the glandular cells of the endocervix. A rare subtype of adenocarcinoma, known as clear cell adenocarcinoma (also called clear cell carcinoma or mesonephroma), occurs infrequently [14].

One of the primary causes of cervical cancer is the human papillomavirus (HPV). According to the WHO, there are approximately 200 types of HPV, though not all pose a risk. Among them, 40 types are associated with cervical cancer, and 14 high-risk types (HPV-16, 18, 31, 33, 35, 39, 45, 51, 52, 56, 58, 59, 66, and 68) are particularly significant. Of these, HPV-16 and HPV-18 are the leading causes of cervical cancer [23, 14, 17].

Detecting cervical cancer at an early stage is challenging because early-stage cervical cancer usually has no symptoms. Symptoms often appear only after the cancer has progressed. Early-stage symptoms may include vaginal bleeding between periods, heavier or longer periods than usual, postmenopausal bleeding, vaginal bleeding after sexual intercourse, watery vaginal discharge with a strong odor or containing blood, and pelvic pain or discomfort during sex.

Symptoms of advanced cervical cancer may include those of early-stage cancer, as well as difficulty or pain during bowel movements, rectal bleeding, painful urination, blood in the urine, dull back pain, leg swelling, abdominal pain, and fatigue [14].

Cancer staging describes the extent to which cancer has spread in the body and helps determine the appropriate treatment. In 2018, the FIGO classification was revised to incorporate iconographic and/or anatomopathological data. Stage I refers to tumors confined to the cervix. Stage II extends beyond the cervix but does not reach the pelvic wall or the lower third of the vagina. Stage III involves hydronephrosis or lymph node invasion, and Stage IV refers to cancers that invade adjacent organs (rectum, bladder) (IVA) or present distant metastases (IVB) [14, 21].

Traditionally, the general treatment of cervical cancer has been based on radiotherapy and/or surgery. The use of chemotherapy, especially since the late 1990s, has enhanced treatment effectiveness. Multicenter studies have demonstrated that combining radiotherapy with chemotherapy significantly improves outcomes, including survival rates and the reduction of distant metastases.

While radiochemotherapy has shown significant benefits, including improving overall survival and reducing recurrence rates, it is associated with side effects. In this article, we focus on hematological toxicity as a frequent and undesirable side effect of radiochemotherapy.

The first use of mathematical modeling in epidemiology dates back to 1760 when Daniel Bernoulli used it to demonstrate the effectiveness of variolation in preventing smallpox by reducing mortality and increasing life expectancy [16]. Today, epidemiological modeling is applied to both infectious diseases (e.g., HIV, hepatitis C, influenza) and non-infectious diseases (e.g., cancer). The objectives of epidemiological modeling include describing complex data, identifying fundamental laws governing disease spread, estimating parameters not directly measurable, predicting future disease cases, and optimizing experimental designs. Compartmental models, which classify populations based on infection or disease status, simulate population dynamics over time using theoretical formulations.

In the context of cervical cancer, several researchers have developed models to analyze its dynamics. For example, Abdulsamed Engida Sado [6] proposed a compartmental model to

examine the impact of HPV vaccination on controlling and reducing cervical cancer. Other studies, such as [17], explored the use of fractional-order models to understand memory effects and genotype-related factors in HPV transmission and cervical cancer dynamics.

In this research, we constructed a mathematical model to study cervical cancer dynamics and the hematological toxicity associated with radiochemotherapy. The model comprises five sub-populations: stage I and II (denoted as A), stage III (denoted as B), stage IV (denoted as C), recovered patients (denoted as D), and patients with hematological toxicity (denoted as H). The model is represented by a system of differential equations. The stability analysis of the equilibrium point helps determine the dynamics of these sub-populations over time, and numerical simulations validate the results of the dynamic analysis.

Using this model, we aim to better understand the mechanisms leading to hematological toxicity after radiochemotherapy and to improve treatment strategies to reduce these side effects.

2. FORMULATION OF THE MODEL

During the construction of the model, we considered a population of patients suffering from cervical cancer in a hospital setting. It is assumed that all individuals are diagnosed with cervical cancer upon their initial arrival at the hospital, and patients are classified into sub-populations based on the stage of their disease.

Throughout the hospital treatment period, it is assumed that all patients, regardless of their cancer stage, undergo radiochemotherapy. Over time, patients may experience changes in their cancer stages, leading to variations in the number of individuals in each sub-population. Specifically, some patients may progress to more severe stages of the disease, others may recover without experiencing adverse effects, and some may develop hematological toxicity as a result of the radiochemotherapy treatment.

These variations in the dynamics of the sub-populations are represented in a compartmental diagram to illustrate the transitions between different states.

We developed a model comprising five compartments representing sub-populations of patients with cervical cancer, classified according to disease stages. Each sub-population is associated with one of the variables A, B, C, D, and H. Sub-population A includes patients with stage I and II cervical cancer, B represents patients with stage III cancer, and C corresponds to

patients with stage IV cancer. Sub-population D comprises patients who have been cured following Radio-Chemotherapy, while H represents patients who have developed hematological toxicity.

Below, Figure 1 illustrates the compartmental diagram, which classifies the sub-populations according to the stages of cervical cancer. The dynamics of these sub-populations are described by a system of differential equations, as expressed in equation (1).

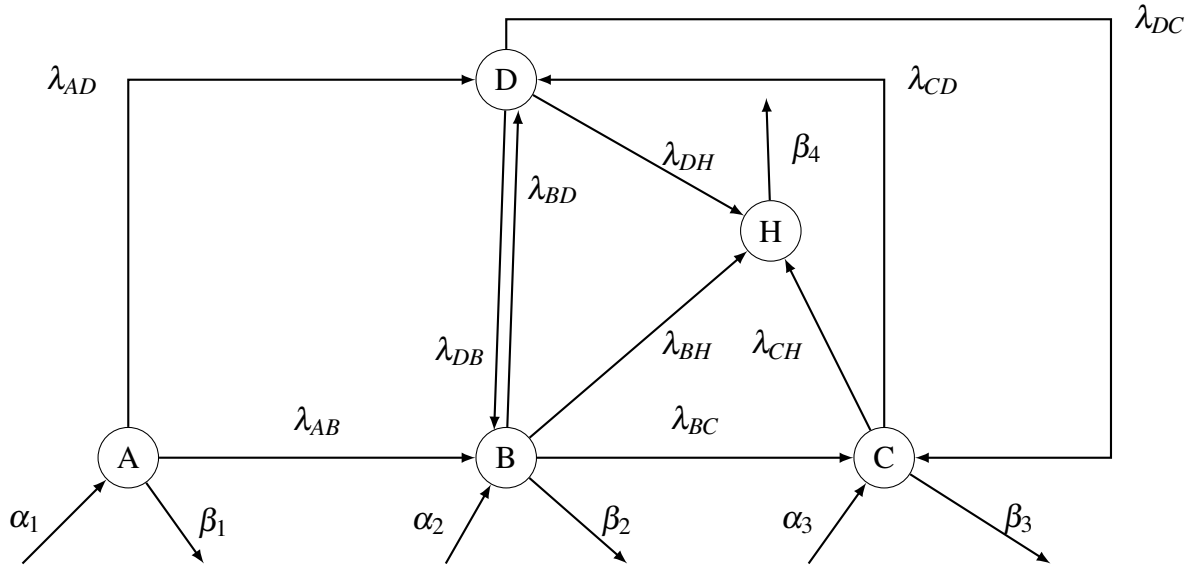

FIGURE 1. Compartment Diagram

$$
(1) \qquad \begin{cases} \dfrac{dA}{dt} = \alpha_1 - \lambda_{AB}A - \lambda_{AD}A - \beta_1 A \\ \dfrac{dB}{dt} = \alpha_2 + \lambda_{AB}A + \lambda_{DB}D - \lambda_{BD}B - \lambda_{BC}B - \lambda_{BH}B - \beta_2 B \\ \dfrac{dC}{dt} = \alpha_3 + \lambda_{BC}B + \lambda_{DC}D - \lambda_{CD}C - \lambda_{CH}C - \beta_3 C \\ \dfrac{dD}{dt} = \lambda_{AD}A + \lambda_{BD}B + \lambda_{CD}C - \lambda_{DB}D - \lambda_{DC}D - \lambda_{DH}D \\ \dfrac{dH}{dt} = \lambda_{DH}D + \lambda_{BH}B + \lambda_{CH}C - \beta_4 H \end{cases}
$$

with a vector's initial condition being appropriate

$$A(0) = A_0 > 0;\ B(0) = B_0 > 0;\ C(0) = C_0 > 0;\ D(0) = D_0 \geq 0;\ H(0) = H_0 \geq 0.$$

All parameters described in TABLE (1) are assumed to have positive values.

Stage I and II patients are placed in the same sub-population because their numbers upon arrival at the hospital are small compared to the other sub-populations. Therefore, patients who are diagnosed for the first time with stage I and II cancer are placed in the compartment with a rate α_1. After receiving a combined treatment of chemotherapy and radiotherapy, patients in sub-population A have two possible outcomes: either they recover at a rate λ_{AD}, or their condition progresses to stage III cancer at a rate λ_{AB}. Additionally, patients in this compartment may die due to cervical cancer at a rate β_1.

In many cases, patients are diagnosed with stage III cancer, so they are placed in compartment B at a rate α_2. After undergoing chemo-radiotherapy, they may recover at a rate λ_{BD} or progress to stage IV cancer, moving to compartment C at a rate λ_{BC}. Patients in this compartment may also die at a rate β_2. Since patients in stage III receive a higher treatment dose compared to those in compartment A, they may develop hematological toxicity at a rate λ_{BH}.

Patients diagnosed for the first time with an advanced stage of cancer are classified in sub-population C at a rate α_3. After undergoing intensive chemo-radiotherapy, these patients may recover at a rate λ_{CD} or develop hematological toxicity at a rate λ_{CH}. Sub-population C also experiences deaths due to cervical cancer at a rate β_3.

Sub-population D consists of patients cured from sub-populations A, B, and C. Patients in this sub-population may either remain cured indefinitely or relapse. This means they can re-enter sub-population B at a rate λ_{DB} or sub-population C at a rate λ_{DC}. Over time, patients in sub-population D may also develop hematological toxicity at a rate λ_{DH}. Patients who suffer from hematological toxicity can die at a rate β_4.

TABLE 1. The description of the parameters

Parameter	Description
α_1	the rate of new cases suffering from stage IA ,IB and IIA, IIB cervical cancer
α_2	the rate of new cases suffering from stage III cervical cancer
α_3	the rate of new cases suffering from stage IV cervical cancer
λ_{AB}	the growth rate from stage I or II to stage III
λ_{BC}	the growth rate from stage III to stage IV
λ_{AD}	Rate of cured stage I or II patients
λ_{BD}	the number of cured stage III patients
λ_{CD}	the number of cured stage IV patients
λ_{BH}	Rate of stage III patients experiencing hematologic toxicity after Radio-Chemotherapy
λ_{CH}	Rate of stage IV patients experiencing hematologic toxicity after Radio-Chemotherapy
λ_{DH}	Rate of disease-free patients with hematological toxicity
λ_{DB}	Rate of patients cured of disease that returns to stage III
λ_{DC}	Rate of patients cured of disease that returns to stage IV
β_1	Mortality rate of patients with stage I or II cancer
β_2	Mortality rate of patients with stage III cancer
β_3	Mortality rate of patients with stage IV cancer
β_4	Mortality rate of patients with hematological toxicity

3. MODEL ANALYSIS

This part is dedicated to the study of the stability of the system of equations (1), focusing on the existence and stability of the equilibrium points.

3.1. Existence and Uniqueness. We study the existence and uniqueness of model (1). To do this, we present model (1) in the following form:

$$A'(t) = F_1(t,A,B,C,D,H)$$

$$B'(t) = F_2(t,A,B,C,D,H)$$

$$C'(t) = F_3(t,A,B,C,D,H)$$

$$D'(t) = F_4(t,A,B,C,D,H)$$

$$H'(t) = F_5(t,A,B,C,D,H)$$

We choose the norm defined by:

$$\|A\|_\infty = \sup_{s\in I}|A(t)|,$$

where $I \subseteq [0,T]$.

We assume that $A(t)$, $B(t)$, $C(t)$, $D(t)$, and $H(t)$ are all bounded in $[0,T]$ for all $s \in [0,T]$, and there exist $i_1,\ldots,i_5$ such that:

$$\|A\|_\infty < i_1, \quad \|B\|_\infty < i_2, \quad \|C\|_\infty < i_3, \quad \|D\|_\infty < i_4 \quad \textit{and} \quad \|H\|_\infty < i_5.$$

Here, we will show that $F_1,\ldots,F_5$ are bounded.

$$\begin{aligned}
|F_1(t,A,B,C,D,H)| &= |\alpha_1 - \eta_1 A| \\
&< \alpha_1 + \eta_1|A| \\
&< \alpha_1 + \eta_1 \sup_N |A| \\
&< \alpha_1 + \eta_1\|A\| \\
&< \alpha_1 + \eta_1 i_1 < \infty
\end{aligned}$$

With : $N = s \in [0,T]$, and $\eta_1 = \lambda_{AB} + \lambda_{AD} + \beta_1$.

In the same way, we can easily prove the following result:

$$\begin{aligned}
|F_2(t,A,B,C,D,H)| &= |\alpha_2 + \lambda_{AB}A + \lambda_{DB}D - \eta_2 B| \\
&< \alpha_1 + \lambda_{AB}|A| + \lambda_{DB}|D| + \eta_2|B| \\
&< \alpha_1 + \lambda_{AB}\|A\| + \lambda_{DB}\|D\| + \eta_2\|B\| \\
&< \alpha_1 + \lambda_{AB}i_1 + \lambda_{DB}i_4 + \eta_2 i_2 < \infty
\end{aligned}$$

Where, $\eta_2 = \lambda_{BD} + \lambda_{BC} + \lambda_{BH} + \beta_2$

$$\begin{aligned}
|F_3(t,A,B,C,D,H)| &= |\alpha_3 + \lambda_{BC}B + \lambda_{DC}D - \eta_3 C| \\
&< \alpha_3 + \lambda_{BC}|B| + \lambda_{DC}|D| + \eta_3|C| \\
&< \alpha_3 + \lambda_{BC}\|B\| + \lambda_{DC}\|D\| + \eta_3\|C\|
\end{aligned}$$

$$< \alpha_3 + \lambda_{BC} i_2 + \lambda_{DC} i_4 + \eta_3 i_3 < \infty$$

Where $\eta_3 = \lambda_{CD} + \lambda_{CH} + \beta_3$.

$$\begin{aligned} |F_4(t,A,B,C,D,H)| &= |\lambda_{AD}A + \lambda_{BD}B + \lambda_{CD}C - \eta_4 D| \\ &< \lambda_{AD}|A| + \lambda_{BD}|B| + \lambda_{CD}|C| + \eta_4|D| \\ &< \lambda_{AD}\|A\| + \lambda_{BD}\|B\| + \lambda_{CD}\|C\| + \eta_4\|D\| \\ &< \lambda_{AD} i_1 + \lambda_{BD} i_2 + \lambda_{CD} i_3 + \eta_4 i_4 < \infty \end{aligned}$$

Where $\eta_4 = \lambda_{DB} + \lambda_{DC} + \lambda_{DH}$,

$$\begin{aligned} |F_5(t,A,B,C,D,H)| &= |\lambda_{DH}D + \lambda_{BH}B + \lambda_{CH}C - \eta_5 H| \\ &< \lambda_{DH}|D| + \lambda_{BH}|B| + \lambda_{CH}|C| + \eta_5|H| \\ &< \lambda_{DH}\|D\| + \lambda_{BH}\|B\| + \lambda_{CH}\|C\| + \eta_5\|H\| \\ &< \lambda_{DH} i_4 + \lambda_{BH} i_2 + \lambda_{CH} i_3 + \eta_5 i_5 < \infty \end{aligned}$$

Where $\eta_5 = \beta_4$, it therefore follows that $A(t)$, $B(t)$, $C(t)$, $D(t)$, and $H(t)$ are bounded, and there exist $s_1, \ldots, s_5$ such that:

$$\begin{aligned} \sup_N |F_1(t,A,B,C,D,H)| &< s_1 \\ \sup_N |F_2(t,A,B,C,D,H)| &< s_2 \\ \sup_N |F_3(t,A,B,C,D,H)| &< s_3 \\ \sup_N |F_4(t,A,B,C,D,H)| &< s_4 \\ \sup_N |F_5(t,A,B,C,D,H)| &< s_5 \end{aligned}$$

We will also show that:

$$\begin{aligned} |F_1(t,A_1,B,C,D,H) - F_1(t,A_2,B,C,D,H)| &= |\alpha_1 - \eta_1 A_1 - \alpha_1 + \eta_1 A_2| \\ &= |\eta_1(A_2 - A_1)| \\ &< \eta_1 |A_1 - A_2| \end{aligned}$$

Likewise, we prove that:

$$|F_2(t,A,B_2,C,D,H) - F_2(t,A,B_2,C,D,H)| < \eta_2|B_1 - B_2|$$

$$|F_3(t,A,B,C_1,D,H) - F_3(t,A,B,C_2,D,H)| < \eta_3|C_1 - C_2|$$

$$|F_4(t,A,B,C,D_1,H) - F_4(t,A,B,C,D_2,H)| < \eta_4|D_1 - D_2|$$

$$|F_5(t,A,B,C,D,H_1) - F_5(t,A,B,C,D,H_2)| < \eta_5|H_1 - H_2|$$

From this, we can conclude that model (1) has a unique system of solutions.

3.2. Equilibrium Point. According to the system of equations (1) we found an equilibrium point denoted $E^* = (A^*, B^*, C^*, D^*, H^*)$ defined by:

$$A^* = \frac{\alpha_1}{\eta_1}, \qquad B^* = \frac{\alpha}{\eta_1 \mu}, \qquad C^* = \frac{\beta}{\eta_1 \mu\ \gamma_1}, \qquad D^* = \frac{\delta}{\eta_1 \mu\ \gamma_2}, \qquad H^* = \frac{\xi}{\eta_1 \mu\ \gamma_3}.$$

where:

$$\eta_1 = \lambda_{AB} + \lambda_{AD} + \beta_1, \quad \eta_2 = \lambda_{BD} + \lambda_{BC} + \lambda_{BH} + \beta_2, \quad \eta_3 = \lambda_{CD} + \lambda_{CH} + \beta_3,$$

$$\eta_4 = \lambda_{DB} + \lambda_{DC} + \lambda_{DH}, \quad \textit{and} \quad \eta_5 = \beta_4$$

$$\begin{aligned}
\alpha =& \eta_1\alpha_2(\lambda_{CD}(\lambda_{DB} + \lambda_{DH}) + \lambda_{CH}(\lambda_{DB} + \lambda_{DC} + \lambda_{DH}) + \eta_4\beta_3) + \alpha_1\lambda_{AB}(\lambda_{CD}(\lambda_{DB} + \lambda_{DH}) \\
&+ \eta_4(\lambda_{Ch} + \beta_3)) + \alpha_1\eta_3\lambda_{DB}\lambda_{AD} + \alpha_3\eta_1\lambda_{DB}\lambda_{CD}. \\
\mu =& \lambda_{DH}\lambda_{CD}(\lambda_{BD} + \lambda_{BC}) + (\lambda_{DH} + \lambda_{DC})(\lambda_{CH} + \lambda_{BD} + \beta_3\lambda_{BD}) + \eta_4(\lambda_{BC}\lambda_{CH} + \beta_3\lambda_{BC} \\
&+ \lambda_{BH}(\lambda_{CH} + \beta_3) + \beta_2(\lambda_{CH} + \beta_2))\lambda_{BH}\lambda_{CD}(\lambda_{DB} + \lambda_{DH}) + \beta_2\lambda_{CD}(\lambda_{DB} + \lambda_{BH}) \\
\beta =& \eta_1\eta_4\alpha_3\mu + (\eta_4\lambda_{BC} + \lambda_{BD}\lambda_{DC})\alpha + \alpha_1\mu\lambda_{DC}\lambda_{AD} \\
\gamma_1 =& \lambda_{CD}(\lambda_{DB} + \lambda_{DH}) + \lambda_{CH}\eta_4 + \beta_3\eta_4 \\
\gamma_2 =& \gamma_1\eta_4 \\
\delta =& \eta_1\gamma_1\alpha_1\mu\lambda_{AD} + \lambda_{BD}\gamma_1\alpha + \lambda_{CD}\beta \\
\gamma_3 =& \gamma_2\eta_5 \\
\xi =& \lambda_{DH}\delta + \lambda_{BH}\gamma_2\alpha + \eta_4\lambda_{CH}\beta
\end{aligned}$$

These equilibrium points are critical to understanding the cervical cancer model because they provide important information about the environmental factors necessary for the spread of cancer. The study's conclusions are as follows:

Theorem 3.1. *An equilibrium point exists according to the system of equations (1) for cervical cancer without any conditions.*

3.3. Analyzing the Stability of Equilibrium Points. In this part, we will study the stability of the equilibrium point. To do this, we will first rewrite the equation in the following matrix form:

$$F = KG + H$$

where

$$F = \begin{bmatrix} \dot{A} \\ \dot{B} \\ \dot{C} \\ \dot{D} \\ \dot{H} \end{bmatrix}; \quad K = \begin{bmatrix} -\eta_1 & 0 & 0 & 0 & 0 \\ \lambda_{AB} & -\eta_2 & 0 & \lambda_{DB} & 0 \\ 0 & \lambda_{BC} & -\eta_3 & \lambda_{DC} & 0 \\ \lambda_{AD} & \lambda_{BD} & \lambda_{CD} & -\eta_4 & 0 \\ 0 & \lambda_{BH} & \lambda_{CH} & \lambda_{DH} & -\eta_5 \end{bmatrix}; \quad G = \begin{bmatrix} A \\ B \\ C \\ D \\ H \end{bmatrix}; \quad H = \begin{bmatrix} \alpha_1 \\ \alpha_2 \\ \alpha_3 \\ 0 \\ 0 \end{bmatrix}$$

Regarding the characteristic equation, we have calculated it using the following formula:

$$P(\lambda) = \begin{vmatrix} -\eta_1 - \lambda & 0 & 0 & 0 & 0 \\ \lambda_{AB} & -\eta_2 - \lambda & 0 & \lambda_{DB} & 0 \\ 0 & \lambda_{BC} & -\eta_3 - \lambda & \lambda_{DC} & 0 \\ \lambda_{AD} & \lambda_{BD} & \lambda_{DC} & -\eta_4 - \lambda & 0 \\ 0 & \lambda_{BH} & \lambda_{CH} & \lambda_{DH} & -\eta_5 - \lambda \end{vmatrix}$$

We get,

$$P(\lambda) = -(\eta_1 + \lambda)(\eta_5 + \lambda)(\lambda^3 + p_1\lambda^2 + p_2\lambda + p_3) \tag{2}$$

We can easily show that equation (2) has five eigenvalues: $-\lambda_1$, $-\lambda_2$, and the other three eigenvalues are the roots of the following equation:

$$\lambda^3 + p_1\lambda^2 + p_2\lambda + p_3 = 0$$

where the coefficients are:

$$\begin{cases} p_1 = \eta_2 + \eta_3 + \eta_4. \\ p_2 = \eta_2\eta_3 + \eta_4\eta_2 + \eta_4\eta_3 - \lambda_{DC}\lambda_{CD} - \lambda_{DB}\lambda_{BD}. \\ p_3 = \eta_2\eta_3\eta_4 - \eta_2\lambda_{DC}\lambda_{CD} - \eta_3\lambda_{DB}\lambda_{BD} - \lambda_{BC}\lambda_{DB}\lambda_{CD} \end{cases}$$

In this part, we worked with the Routh-Hurwitz criterion [4, 5] to check the stability of the equilibrium points, which uses the characteristic equation obtained previously.

Routh's table allows us to study their nature, and then we have:

$$\begin{array}{c|ccc} \lambda^3 & 1 & p_2 & 0 \\ \lambda^2 & p_1 & p_3 & 0 \\ \lambda^1 & b_1 & 0 & \\ \lambda^0 & p_3 & & \end{array}$$

with $b_1 = \frac{p_1 p_2 - p_3}{p_1}$. According to Routh's table, we found that the coefficients are all positive in the first column, which means that all the real eigenvalues are negative.

We can easily show that p_1, b_1, and p_3 are all positive. Therefore, according to the Routh-Hurwitz criterion, it follows that the system of equations (1) is locally asymptotically stable.

4. Numerical Simulation and Discussion

This section concerns the numerical simulation, where we will examine the results already found in the previous section using numerical simulations. We carried out the numerical simulations with the following parameter values: $\alpha_1 = 5$; $\alpha_2 = 20$; $\alpha_3 = 11$; $\beta_1 = 0.5$; $\beta_2 = 0.8$; $\beta_3 = 0.4$; $\beta_4 = 0.5$; $\lambda_{AB} = 0.56$; $\lambda_{AD} = 0.63$; $\lambda_{BC} = 0.12$; $\lambda_{BD} = 0.35$; $\lambda_{BH} = 0.41$; $\lambda_{CD} = 0.32$; $\lambda_{CH} = 0.52$; $\lambda_{DB} = 0.42$; $\lambda_{DC} = 0.42$; $\lambda_{DH} = 0.5$. Based on the values of the previous parameters, we found the equilibrium point $E^*(A^*, B^*, C^*, D^*, H^*)$ where: $A^* = 3$, $B^* = 1$, $C^* = 14$, $D^* = 10$, $H^* = 38$. Thus, the results of the numerical simulation are presented in Figure 2.

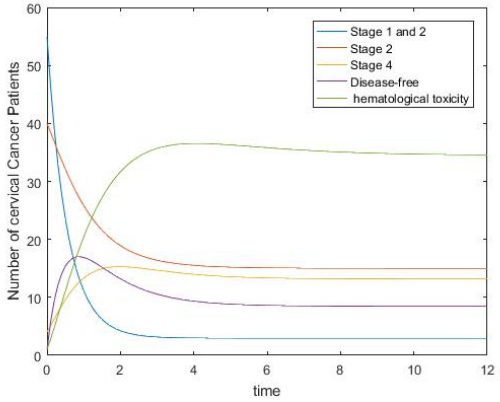

FIGURE 2. The numerical simulation results of the model with initial conditions $(A_0, B_0, C_0, D_0, H_0) = (55, 40, 4, 1, 1)$.

From Figure 2, it turns out that the equilibrium conditions begin from the sixth period. The Phase I and II sub-populations are reduced from an initial case of 55 patients to 3 patients at steady state. Similarly, the stage III sub-population, initially at 40 patients, decreased to 17 under steady-state conditions. For stage IV patients, we notice a slight increase from 4 to 10 people in equilibrium conditions. The cured sub-population increased significantly from 1 to 14 patients. The sub-population affected by hematological toxicity experienced a substantial increase, from 1 patient at baseline to 38 patients at steady state. These results are considered preliminary simulations.

In the following two simulations, we reduced the relapse rate and the hematological toxicity rate.

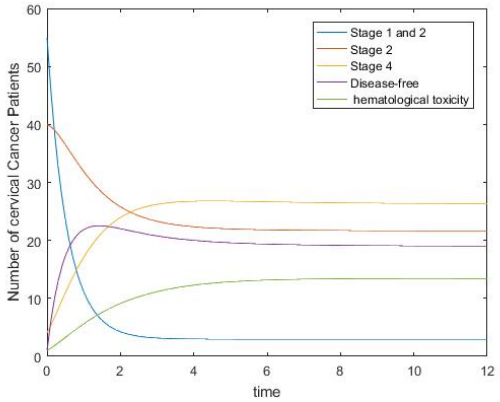

FIGURE 3. The numerical simulation results of the model with $\lambda_{BH} = 0.1$ and $\lambda_{CH} = 0.1$.

After reducing the hematological toxicity rates λ_{BH} and λ_{CH} to both 0.1, we see the results of this simulation in Figure 3. It is noted that the disease-free sub-population amounts to 20 patients. Additionally, a significant result was observed in patients affected by hematological toxicity. The rate of patients in this sub-population fell to 12 in stable condition. Concerning the stage IV sub-population, there was a notable increase that was not observed in the initial simulation. However, for the other sub-populations, we found the same results as those of the initial simulation.

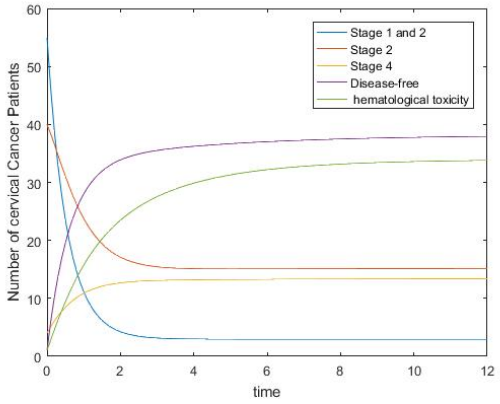

FIGURE 4. The numerical simulation results of the model with $\lambda_{DB} = 0.1$, $\lambda_{DC} = 0.1$, and $\lambda_{DH} = 0.1$.

Figure 4 illustrates the results of the simulation aimed at reducing the relapse rates λ_{DB}, λ_{DC}, and λ_{DH} to 0.1. A significant increase was noted in people without the disease, up to 38 cases. At the same time, the number of patients affected by hematological toxicity also increased significantly. On the other hand, there was no change in the other sub-populations, as the results remained the same as those of the first simulation.

5. CONCLUSION

In this article, we developed a mathematical model consisting of five compartments. The first three compartments represent sub-populations affected by cervical cancer, classified according to stages I, II, III, and IV. One compartment represents patients who have been cured of the disease, while the final compartment contains patients who have developed hematological toxicity. We then performed a dynamic analysis to study the dynamics of affected individuals

in each sub-population over time. Based on the results of the dynamic analysis, we identified an equilibrium point that is stable under all conditions. Additionally, we conducted numerical simulations to verify the solutions around the equilibrium point.

The results of the numerical simulations indicate that the population will stabilize over time, regardless of the initial conditions, provided all parameters remain constant. This demonstrates that the equilibrium point of the system is stable under these conditions. However, when we minimized the relapse rate, we observed a negative outcome: an increase in the sub-populations presenting hematological toxicity. On the other hand, reducing the rates of hematological toxicity yielded positive results. Specifically, the number of disease-free sub-populations increased, while the number of sub-populations presenting hematological toxicity decreased.

Based on the simulation results, we propose an optimal solution to reduce the number of patients suffering from hematological toxicity and increase the number of patients who fully recover from the disease after receiving radio-chemotherapy treatment. This solution involves reducing the hematological toxicity rates in stage III and IV sub-populations

CONFLICT OF INTERESTS

The authors declare that there is no conflict of interests.

REFERENCES

[1] Information Centre on HPV and Cancer, Morocco: Human Papillomavirus and Related Cancers, Fact Sheet 2023, (2023). https://hpvcentre.net/statistics/reports/MAR_FS.pdf.

[2] C. Beskow, A. Ågren-Cronqvist, R. Lewensohn, I. Toma-Dasu, EP-1142 Bed Dependence of Local Control and Late Toxicity for Cervical Cancer Treated With Radiotherapy and Surgery, Radiother. Oncol. 103 (2012), S439–S440. https://doi.org/10.1016/s0167-8140(12)71475-5.

[3] M. Boily, R.V. Barnabas, M.M. Rönn, C.J. Bayer, C. van Schalkwyk, et al., Estimating the Effect of HIV on Cervical Cancer Elimination in South Africa: Comparative Modelling of the Impact of Vaccination and Screening, eClinicalMedicine 54 (2022), 101754. https://doi.org/10.1016/j.eclinm.2022.101754.

[4] M. El Karchani, N.I. Fatmi, K. Mouden, Analysing the Effect of Trastuzumab Treatment on Breast Cancer Stages and Cardiac Function: A Mathematical Modeling and Numerical Simulation, Commun. Math. Biol. Neurosci. 2023 (2023), 47. https://doi.org/10.28919/cmbn/7970.

[5] M. El Karchani, N.I. Fatmi, K. Mouden, Quantifying the Impact of Immunotherapy Response of Breast Cancer Stages: A Computational Approach for Mathematical Model and Numerical Simulation, Commun. Math. Biol. Neurosci. 2023 (2023), 138. https://doi.org/10.28919/cmbn/8341.

[6] A. Engida Sado, Mathematical Modeling of Cervical Cancer with HPV Transmission and Vaccination, Sci. J. Appl. Math. Stat. 7 (2019), 21–25. https://doi.org/10.11648/j.sjams.20190702.13.

[7] G. Liu, N.R. Mugo, C.J. Broshkevitch, D.W. Rao, M. Onono, et al., Impact of Catch-Up Human Papillomavirus Vaccination on Cervical Cancer Incidence in Kenya: A Mathematical Modeling Evaluation of HPV Vaccination Strategies in the Context of Moderate HIV Prevalence, eClinicalMedicine 45 (2022), 101306. https://doi.org/10.1016/j.eclinm.2022.101306.

[8] G. Liu, Y. Feng, J. Li, H. Huang, T. Wan, et al., A Novel Combo of Niraparib and Anlotinib in Platinum-Resistant Ovarian Cancer, the Final Efficacy and Safety Report of ANNIE Study, a Phase II, Multi-Center Trial (LBA 2), Gynecol. Oncol. 166 (2022), S47. https://doi.org/10.1016/s0090-8258(22)01291-4.

[9] M.I.A. Fathoni, Gunardi, F.A. Kusumo, S.H. Hutajulu, Mathematical Model Analysis of Breast Cancer Stages with Side Effects on Heart in Chemotherapy Patients, AIP Conf. Proc. 2192 (2019), 060007. https://doi.org/10.1063/1.5139153.

[10] L. Guo, W. Wang, X. Xie, S. Wang, Y. Zhang, Machine Learning for Genetic Prediction of Chemotherapy Toxicity in Cervical Cancer, Biomed. Pharmacother. 161 (2023), 114518. https://doi.org/10.1016/j.biopha.2023.114518.

[11] L.W. Kivuti-Bitok, G.P. Pokhariyal, G. McDonnell, R. Abdul, A Mathematical Model of Cervical Cancer in Kenya, Int. J. Sci. Res. 4 (2015), 458–465.

[12] C. Marchetti, A. Fagotti, V. Tombolini, G. Scambia, F. De Felice, Survival and Toxicity in Neoadjuvant Chemotherapy Plus Surgery Versus Definitive Chemoradiotherapy for Cervical Cancer: A Systematic Review and Meta-Analysis, Cancer Treat. Rev. 83 (2020), 101945. https://doi.org/10.1016/j.ctrv.2019.101945.

[13] M.T. Segni, H.F. Demissie, D.M. Tadesse, R. Amdemichael, Y.T. Mamo, A. Worku, Level of Knowledge and Associated Factor Toward Cervical Cancer among Women Age (21-64) Years Visiting Health Facilities in Gulele Sub-City Addis Ababa Ethiopia, J. Pancreas 18 (2017), 44–48.

[14] National Cancer Institute, What Is Cervical Cancer?, (2023). https://www.cancer.gov/types/cervical.

[15] D.M. Parkin, S.M. Moss, An Evaluation of Screening Policies for Cervical Cancer in England and Wales Using a Computer Simulation Model., J. Epidemiol. Community Health 40 (1986), 143–153. https://doi.org/10.1136/jech.40.2.143.

[16] P.J. White, Mathematical Models in Infectious Disease Epidemiology, in: Infectious Diseases, Elsevier, 2017: pp. 49–53.e1. https://doi.org/10.1016/B978-0-7020-6285-8.00005-8.

[17] A.R. Butt, A. Ahmad Saqib, A.S. Alshomrani, A. Bakar, M. Inc, Dynamical Analysis of a Nonlinear Fractional Cervical Cancer Epidemic Model with the Nonstandard Finite Difference Method, Ain Shams Eng. J. 15 (2024), 102479. https://doi.org/10.1016/j.asej.2023.102479.

[18] R. Iskandar, K. Taghavi, N. Low, W.M. Bramer, M. Egger, et al., Mathematical Models for Evaluating Effectiveness and Cost-Effectiveness of Cervical Cancer Control Policies in Populations Including Women Living with Human Immunodeficiency Virus: A Scoping Review, Value Health Reg. Issues 32 (2022), 39–46. https://doi.org/10.1016/j.vhri.2022.07.001.

[19] D. Singh, J. Vignat, V. Lorenzoni, M. Eslahi, O. Ginsburg, et al., Global Estimates of Incidence and Mortality of Cervical Cancer in 2020: A Baseline Analysis of the WHO Global Cervical Cancer Elimination Initiative, Lancet Glob. Health 11 (2023), e197–e206. https://doi.org/10.1016/s2214-109x(22)00501-0.

[20] M.S. Ali, M.M. Hossain, M.A. Kona, K.R. Nowrin, M.K. Islam, An Ensemble Classification Approach for Cervical Cancer Prediction Using Behavioral Risk Factors, Healthc. Anal. 5 (2024), 100324. https://doi.org/10.1016/j.health.2024.100324.

[21] K. van Kol, R. Ebisch, M. van der Aa, H. Wenzel, J. Piek, et al., The Prognostic Value of the Presence of Pelvic And/or Para-Aortic Lymph Node Metastases in Cervical Cancer Patients; the Influence of the New FIGO Classification (Stage IIIC), Gynecol. Oncol. 171 (2023), 9–14. https://doi.org/10.1016/j.ygyno.2023.01.023.

[22] Z.W. Florczak, A. Roszak, K. Bratos, H. Wlodarczyk, B. Urbanski, et al., EP-1141 Evaluation of Results for Radiochemotherapy in Womens With Advance Cervical Cancer-Five Years Follow-Up, Radiother. Oncol. 103 (2012), S439. https://doi.org/10.1016/s0167-8140(12)71474-3.

[23] Word Health Organization, Cervical Cancer, 2025. https://www.who.int/news-room/fact-sheets/detail/cervical-cancer.

[24] X. Meng, N. Wang, M. Yu, D. Kong, Z. Zhang, et al., Development of a Nomogram for Predicting Grade 2 or Higher Acute Hematologic Toxicity of Cervical Cancer After the Pelvic Bone Marrow Sparing Radiotherapy, Front. Public Health 10 (2022), 993443. https://doi.org/10.3389/fpubh.2022.993443.